

환원된 산화그래핀/젤라틴 복합필름의 합성과 분석

Guangxin Chen^{*,**}, Congde Qiao^{*,**,*†}, Jing Xu^{**}, and Jinshui Yao^{*}

^{*}School of Materials Science and Engineering, Qilu University of Technology

^{**}Shandong Provincial Key Laboratory of Fine Chemicals, Qilu University of Technology

(2013년 12월 30일 접수, 2014년 2월 1일 수정, 2014년 3월 3일 채택)

Synthesis and Characterization of Reduced Graphene Oxide/Gelatin Composite Films

Guangxin Chen^{*,**}, Congde Qiao^{*,**,*†}, Jing Xu^{**}, and Jinshui Yao^{*}

^{*}School of Materials Science and Engineering, Qilu University of Technology, Jinan 250353, P. R. China

^{**}Shandong Provincial Key Laboratory of Fine Chemicals, Qilu University of Technology, Jinan 250353, P. R. China

(Received December 30, 2013; Revised February 1, 2014; Accepted March 3, 2014)

Abstract: Reduced graphene oxide (RGO) was fabricated using gelatin as a reductant, and it could be stably dispersed in gelatin solution without aggregation. A series of RGO/gelatin composite films with various RGO contents were prepared by a solution-casting method. The structure and thermal properties of the RGO/gelatin composite films were characterized by UV-vis spectroscopy, Fourier transform infrared (FTIR) spectroscopy, X-ray diffraction (XRD), atomic force microscopy (AFM), scanning electron microscopy (SEM), differential scanning calorimeter (DSC) and thermal gravimetric analysis (TGA). The addition of RGO enhances the degree of crosslinking of gelatin films and decreases the swelling ability of the gelatin films in water, indicating that RGO/gelatin composite films have a better wet stability than gelatin films. The glass transition temperature (T_g) of gelatin films is also increased with the incorporation of RGO. The presence of RGO slightly increases the degradation temperature of gelatin films due to the very low content of RGO in the composite films. Since gelatin is a natural and nontoxic biomacromolecule, the RGO/gelatin composite films are expected to have potential applications in the biomedical field.

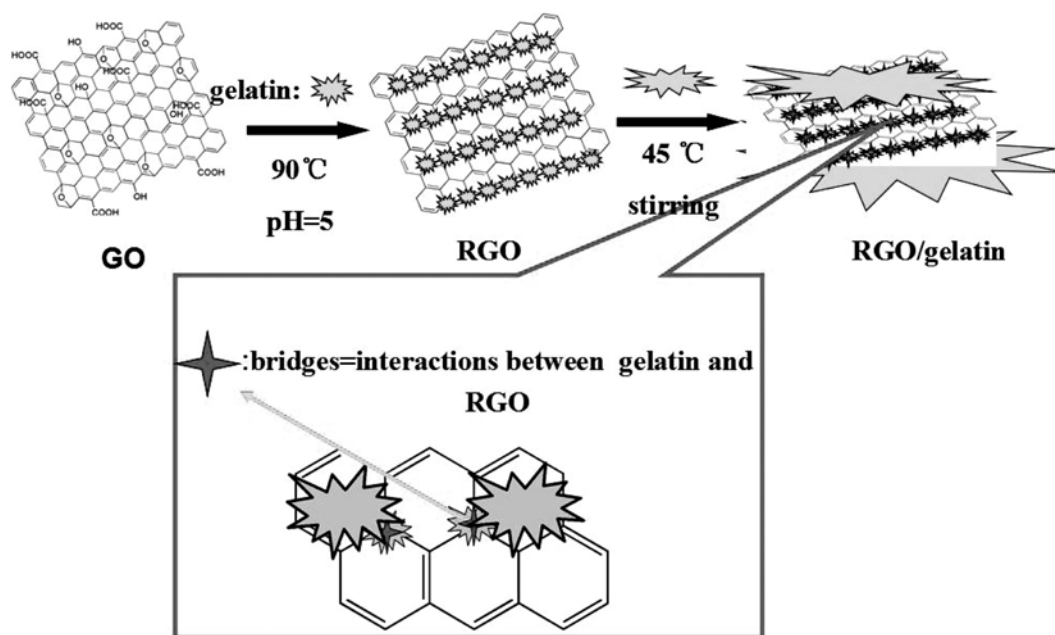
Keywords: reduced graphene oxide, composite materials, thin films, glass transition.

Introduction

Gelatin is a traditional water-soluble biopolymer with distinctive advantages of biocompatibility, nontoxicity, biodegradability and low cost, and is widely used in food, medicine, and photographic fields, such as medicinal capsules,^{1,2} packaging films,^{3,4} nutritional membranes⁵ and hemostatic materials.⁶ However, high hygroscopicity and low strength in the wet state significantly hinder gelatin in biomedical and engineering applications. Thus, modification of gelatin has always been an issue of great interest. For example, the reinforcement using crosslinking effect has been often applied to improve the properties of gelatin. However, the presence of residual crosslinking agents may hamper the application of gelatin due to its toxic side effects.⁷

Graphene, a two-dimensional carbon material, has attracted a great deal of attention recently due to its unique mechanical, electrical and quantum properties.^{8,9} Graphene is expected to be a novel reinforcing material for polymer materials. However, the most commonly used method of preparation of graphene-polymer nanocomposites generally began with graphene oxide.^{10,11} Graphene oxide (GO), a derivative of graphene, has abundant oxygen-containing groups including hydroxyls, epoxides, diols, ketones and carboxyls on the surface.¹⁰ These functional groups can act as interfacial linkers and facilitate stress transfer from the polymer matrix to GO. Moreover, GO is easily produced and can be dispersed in numerous solvents,¹²⁻¹⁴ especially in water. Thus GO is usually used in the composites instead of graphene. Significant improvement in mechanical properties has been reported in GO-reinforced polymers because of its high strength and modulus, large aspect ratio and strong interfacial interactions with polymers.¹⁵⁻¹⁸ Wan¹⁹ prepared free-standing gelatin-GO com-

[†]To whom correspondence should be addressed.
E-mail: cdqiao@spu.edu.cn



Scheme 1. Illustration of the green synthesis of RGO and the composite mechanism of RGO/gelatin.

posite films with exfoliated GO nanosheets, and found that all the tensile strength, modulus and energy at break of gelatin were increased notably with the addition of 1 wt% of GO. The reinforcement of gelatin-GO composite films was resulted from the homogeneous dispersion of GO nanosheets with a high aspect ratio and strong interfacial interactions with gelatin which also resulted in an increase in T_g . However, the properties, such as electrical properties, are not as good as that of graphene, so reduction is often needed to convert insulating GO back to conducting reduced graphene oxide (RGO). Wang²⁰ reported RGO/gelatin composite films with reinforced mechanical strength in both the dry and wet states, and the addition of RGO had no negative effect on compatibility of the gelatin. However, there have been only a few reports about graphene enhanced natural biomaterials and the relationships between structure and properties remain unclear.

In this paper, RGO was fabricated using gelatin as a reductant and a series of RGO/gelatin composite films with varying RGO contents were prepared by a solution-casting method (Scheme 1). The structure and properties of the RGO/gelatin composite films were characterized by UV, Fourier transform infrared (FTIR), X-ray diffraction (XRD), atomic force microscopy (AFM), scanning electron microscopy (SEM), differential scanning calorimeter (DSC) and thermal gravimetric analysis (TGA). The effect of RGO contents on the properties of RGO/gelatin composite films was discussed in detail. Since gelatin is a natural and nontoxic polymer with good biode-

gradability, the RGO/gelatin composite films are expected to have potential applications in biomedical field.

Experimental

Materials. Gelatin type B (gelatin powder from bovine skin, average molecular weight 80000) was purchased from Sigma-Aldrich. Graphite powder, and chemicals including concentrated sulfuric acid, KMnO_4 , NaNO_3 , $\text{K}_2\text{S}_2\text{O}_8$ (99%), concentrated HCl, P_2O_5 (99%), and H_2O_2 were all analytical grade and purchased from Sinopharm Chemical Reagent Co., Ltd. All aqueous solutions were prepared using ultrapure water (18 M Ω) from a Milli-Q system (Millipore). All reagents were used as received without further purification.

Preparation of RGO Aqueous Suspension. GO was prepared by a modified Hummers method.^{21,22} Briefly, concentrated H_2SO_4 was added into a 500 mL flask filled with graphite, followed by the addition of NaNO_3 , and then solid KMnO_4 was gradually added under stirring while the temperature of the mixture was kept below 20 °C. Then the temperature was adjusted to 30 °C, excess distilled water was then added to the mixture and the temperature was increased to 80 °C. Then 30% H_2O_2 was added until the color of the mixture turned to brilliant yellow. The mixture was firstly filtered and washed several times with 8% aqueous HCl to remove metal ions and then washed with distilled water to remove the acid. Finally, the filter cake was dried in air then re-dispersed

into water. The suspended GO sheets were obtained after ultrasonic treatment. In the process of reaction for chemical reduction of GO to RGO, 3 g of gelatin was first added into 100 mL ultrapure water, followed by stirring for 1 h at 50 °C for the complete dissolution of gelatin. Then the GO aqueous dispersion (200 mL with concentration of 0.1 mg/mL) was dropped into the gelatin solution at 90 °C, and the mixture was allowed to react for 24 h under stirring. The as-obtained suspension was centrifuged under 20000 rpm and washed thoroughly with hot water. Finally, the resulting powder was redispersed in ultrapure water to obtain the RGO suspension.

Preparation of RGO/Gelatin Composite Films. A given amount of gelatin and deionized water was added into a beaker at room temperature for half an hour, and then stirred with a magnetic stirrer at 45 °C for 1 h to obtain a gelatin solution with a concentration of 6 wt%. The gelatin solution was divided equally into five parts and the desired amount of RGO aqueous suspension was added to each part to obtain five RGO/gelatin mixtures with RGO contents of 0, 0.1, 0.3, 0.5, and 0.7 wt%, respectively. The mixture was sonicated for 10 min, and then each of the solutions was coated on a polytetrafluoroethylene (PTFE) mold and dried for 48 h in a vacuum oven, yielding the dry RGO/gelatin composite films. For the XRD experiment, the samples were prepared as follows: the gelatin/RGO solution was centrifuged under 20000 rpm and washed thoroughly with hot water. Then, the obtained RGO was dried in the vacuum at 50 °C. Finally, the solid powder was successfully prepared for the XRD experiment.

Characterizations. The UV-vis spectrophotometer (UV-2550, Shimadzu) was used to investigate the optical absorption of the GO and RGO suspensions in the wavelength range of 190–800 nm. FTIR spectra were recorded in the mid-infrared region of 4000–400 cm^{-1} using a Perkin-Elmer Spectromer 100 spectrometer (Perkin-Elmer Company, USA) at room temperature and 50% relative humidity. XRD analysis was conducted with a BDX3300 X-ray diffractometer equipped with a multichannel detector by use of a $\text{CuK}_{\alpha 1}$ ($\lambda=0.15406$ nm) monochromatic X-ray beam. All the samples were measured within 2θ range of 5–60° with a scan rate of 1°/min. AFM images of GO and RGO films were taken in a tapping mode by using a NanoScope III A (Digital Instrument, USA). Image processing and data analysis were performed using nanoscope analysis image processing software version 1.40 provided with the instrument. The samples for the AFM imaging were prepared by drop-casting a diluted suspension onto a cleaned Si substrate. SEM was conducted on a Quanta-200 ESEM (FEI

Co., Holland) using an accelerating voltage of 30 kV. T_g values of gelatin and RGO/gelatin composite films were determined by DSC (Q10, TA instrument). All samples were annealed at 120 °C for 20 min before starting DSC experiments, and then were heated from 40 to 250 °C with a heating rate of 10 °C/min. For the determination of the melt enthalpy of “free water”, the gelatin and RGO/gelatin composite hydrogels samples were quenched to -50 °C with liquid nitrogen before starting heating runs, and then heating was investigated at 10 °C/min to 25 °C. TGA was performed on a SDTQ600 (TA Instrument) from room temperature to 700 °C with a heating rate of 10 °C/min under a nitrogen atmosphere.

Swelling Studies. The dried and accurately weighed samples were immersed in 100 mL distilled water at a preset temperature until the swelling equilibrium was achieved after around 72 h. The equilibrium swelling ratio (ESR) of the films was calculated using eq. (1).

$$\text{ESR} = W_e / W_d \quad (1)$$

where W_e and W_d are the weights of the equilibrated swollen film and the dried film, respectively.

Results and Discussion

Characterization of RGO. Gelatin has not only been used as a functionalized reagent to prevent aggregation, but also acted as a mild reductant for GO.²³ The reduction of GO is presumably resulted from a direct redox reaction between GO and

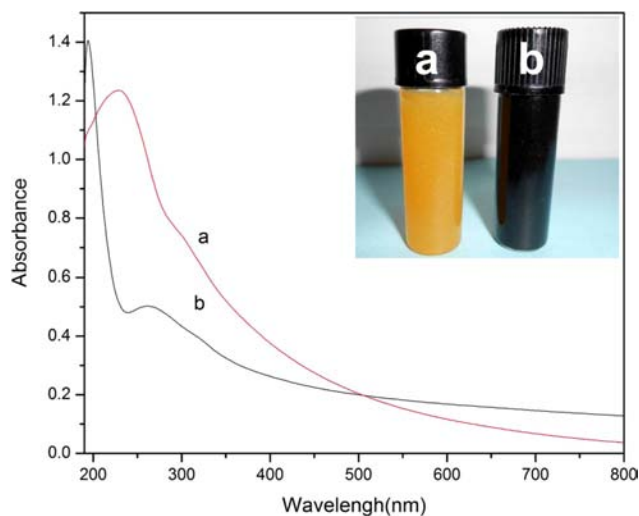


Figure 1. UV-vis absorption spectra and images (inset) of GO (0.1 mg mL^{-1}) (a); RGO/gelatin solutions (0.1 mg mL^{-1}) (b).

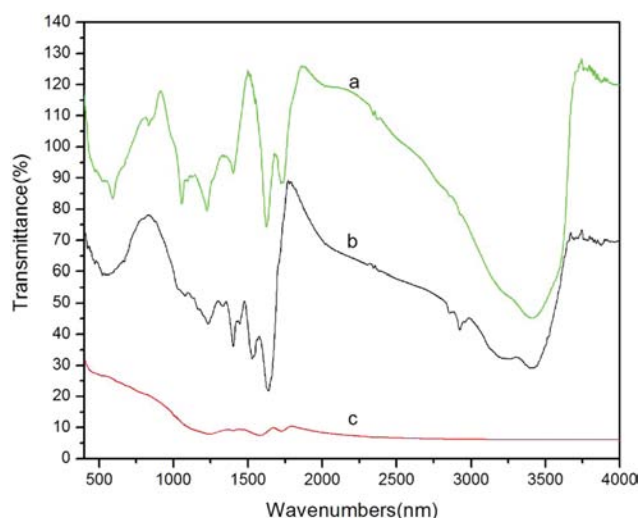


Figure 2. FTIR spectra of GO (a); RGO (b); pure graphene (c).

the -NH_2 groups from gelatin. However, the mechanism for the chemical reduction of GO is not completely clear at present. It needs further study. In Figure 1, a strong absorption at 230 nm is observed for GO, which corresponds to the $\pi \rightarrow \pi^*$ transitions of the aromatic C=C bond. After reduction, the peak at 230 nm was shifted to 265 nm, indicating the restoration of electronic conjugation in RGO occurred.²⁴ Thus, it is concluded that the oxygen groups of GO were reduced by gelatin. Moreover, as shown in the inset of Figure 1, the color changed from bright yellow to black in solution before and after reaction, which also validated the reduction of GO.

The reduction of the oxygen-containing groups in GO by gelatin was also confirmed by the results of FTIR spectroscopy. Figure 2 shows the intensities of the FTIR peaks corresponding to the oxygen functionalities after 24 h reduction of the GO with gelatin,²⁵ such as the C=O stretching vibration peak at 1750 cm^{-1} , the vibration and deformation peaks of O-H groups at 3460 and 1625 cm^{-1} , respectively. The C-O (epoxy) stretching vibration peak at 1225 cm^{-1} and the C-O (alkoxy) stretching peak at 1065 cm^{-1} decreased significantly, and some of them vanished entirely. These observations demonstrated that most of the oxygen-containing groups in the GO were removed, clearly showing the reduction of GO.

XRD is a powerful tool for studying the interlayer changes and the crystalline properties of the synthesized material. A disappearance of characteristic diffraction peak of graphite at 26.4° can be seen in Figure 3, which imply that the complete oxidation of graphite (curve b) occurred. Meanwhile, a new peak is observed at 10.9° when graphite is oxidized to GO, which is due to the intercalation of oxo-groups to the interlayer

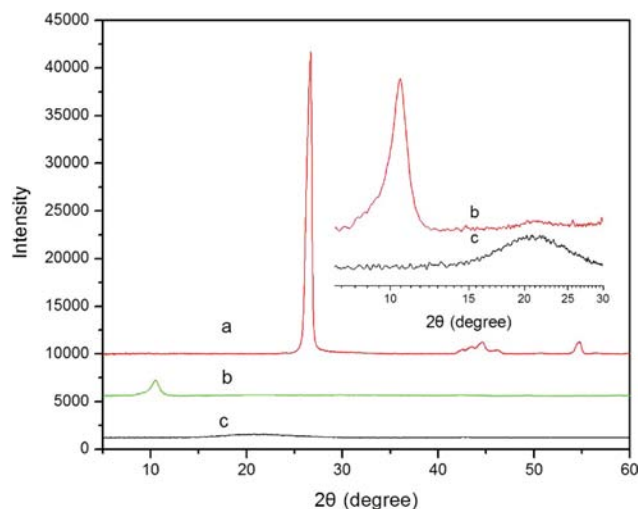


Figure 3. XRD patterns of graphite (a); GO (b); RGO (c).

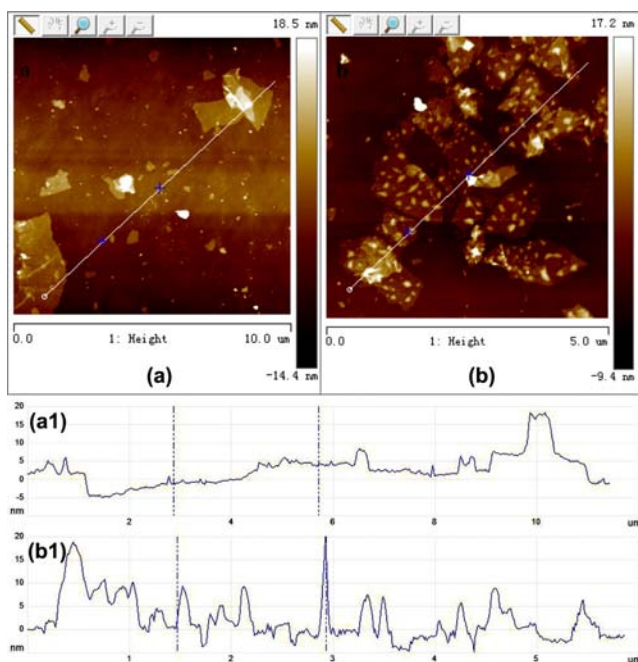


Figure 4. Typical AFM images and cross-section analysis along with the line in AFM images of GO (a, a1); RGO films (b, b1).

of carbon sheets. After the reduction, no obvious peak was detected in the RGO, indicating the complete reduction of GO (curve c).

Atomic force microscopy (AFM) was used to characterize the morphology and thickness of the GO and RGO films. Figure 4 shows the representative AFM images and cross-section analyses along with the line in AFM images of GO and RGO films. The GO nanosheets have a mean thickness of about 0.8 nm, which was larger than the theoretical value of graphene

sheet for the unstripped GO with the presence of covalently bound oxo-groups. After the reduction, the thickness of the obtained RGO nanosheets increased to about 5.0 nm. Although most oxo-groups were removed after the reduction, the thicker RGO nanosheets could be attributed to the attachment of gelatin. Furthermore, as could be observed, the presence of gelatin could prevent the RGO agglomeration, because most of the negative RGO nanosheets were kept independent from each other in the dispersion due to the electrostatic interaction. Therefore, the gelatin could not only act as a reducing reagent, but also plays an important role as a capping reagent for the stabilization of the RGO.

Characterization of RGO/Gelatin Composite Films. Figure 5 shows the SEM images of the cross section of RGO/gelatin composite films with RGO concentration of 0.7 wt%. From Figure 5(a), we can see the RGO/gelatin nanocomposite exhibits a layered morphology without aggregated particles on the surface. In addition, the presence of highly wrinkled edges and flexible sheet-like structures of RGO (Figure 5(b)), which was well dispersed in the gelatin matrix, can lead to increases in both strength and toughness.^{26,27} Similar phenomena have been observed recently in montmorillonite polymer nanocomposites.²⁸

To investigate the interfacial interactions between gelatin and RGO, DSC was applied to measure the glass transition temperature of gelatin and RGO/gelatin composite films (Figure 6). It was found that the glass transition temperature increased from 196.78 °C when the RGO concentration increased from 0 to 0.7 wt%, respectively. The improvement of T_g shows the presence of RGO significantly hinders the mobility of the adsorbed gelatin chains due to the

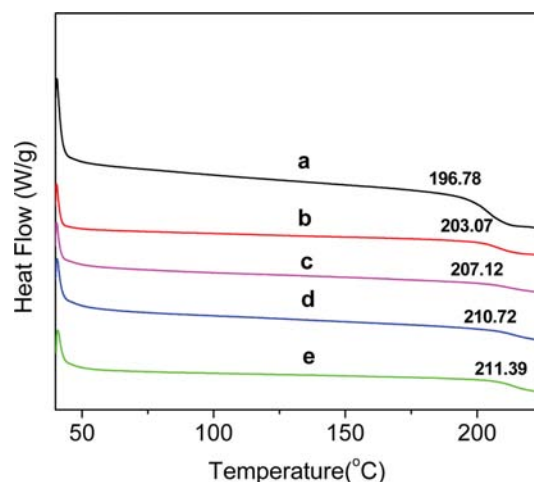


Figure 6. DSC thermograms of gelatin (a); RGO/gelatin composite films with various RGO concentrations of 0.1% (b); 0.3% (c); 0.5% (d); 0.7% (e).

preferable interfacial interactions between the RGO and the polar groups of gelatin and hence indicates strong interfacial interactions in the polymer composites. The DSC results strongly support the previous discussion that suggests good dispersion of RGO in gelatin matrix occurs and therefore a large interfacial surface for interactions between the two components exists. It should be pointed out that all the samples used in the DSC analysis possessed a similar water content of 8 wt%.

The different physical states of water in biomacromolecules have provoked keen interest of many researchers over the past decades. In general, water in a biomacromolecule can be categorized into three types, namely, “free water”, which freezes at the usual freezing point; “intermediate water”, which freezes

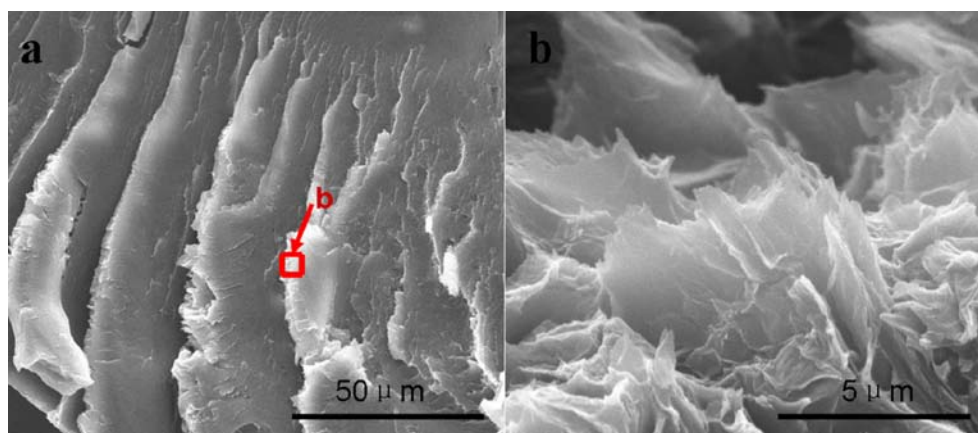


Figure 5. SEM images of RGO/gelatin composite films' cross sections with RGO concentration of 0.7 wt% (a); an image (shown in Figure 5(a)) with high amplification (b).

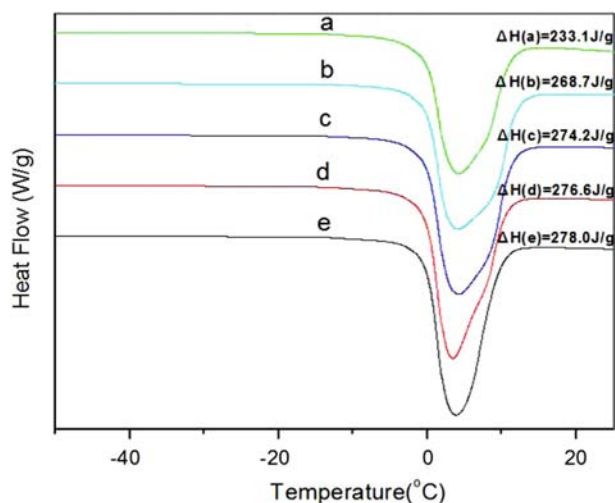


Figure 7. DSC thermograms of RGO/gelatin composite hydrogels with various RGO concentrations of 0.7% (a); 0.5% (b); 0.3% (c); 0.1% (d); 0% (e).

at temperature lower than the usual freezing point; and “unfrozen bound water”, which cannot freeze at the usual freezing point.^{29,30} Figure 7 shows the DSC thermograms of gelatin and RGO/gelatin composite hydrogels with various RGO concentrations. The data of the melt enthalpy of “free water” are listed in the inset of Figure 7. The contents of “free water” in the RGO/gelatin composite hydrogels gradually decrease with an increase in RGO concentrations. It should be noted that all the samples used in the DSC analysis possessed a similar water content of 94 wt%, which excludes the potential influence of water content differences, thus, the other two types of water is gradually increased. It may imply that strong interactions between the RGO sheets and the gelatin molecules exist.

Swelling Behavior of RGO/Gelatin Composite Films.

For the gelatin films, the swelling characteristics are responsible for their various applications. So many studies have been done on the equilibrium swelling behavior of the polymer films. Figure 8 shows the swelling behavior of gelatin and RGO/gelatin composite films with various RGO concentrations. The pure gelatin film has the highest equilibrium swelling ratio, and water absorption capacity of the composite films decreases with an increase in RGO concentrations indicating that RGO/gelatin composite films have a better wet stability than that of gelatin films. This result may be attributed to the physical crosslinking action of the RGO on the gelatin macromolecules which makes the films more stable in an aqueous medium. It is concluded that the addition of RGO increased the degree of crosslinking of gelatin films and it can be verified by the DSC results.

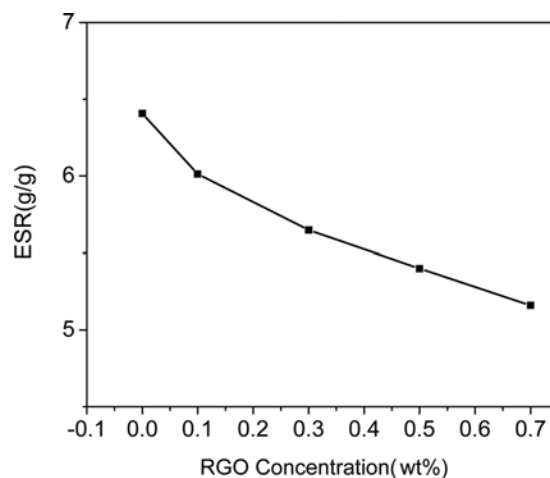


Figure 8. Equilibrium swelling ratio of gelatin and RGO/gelatin composite films with various RGO concentrations.

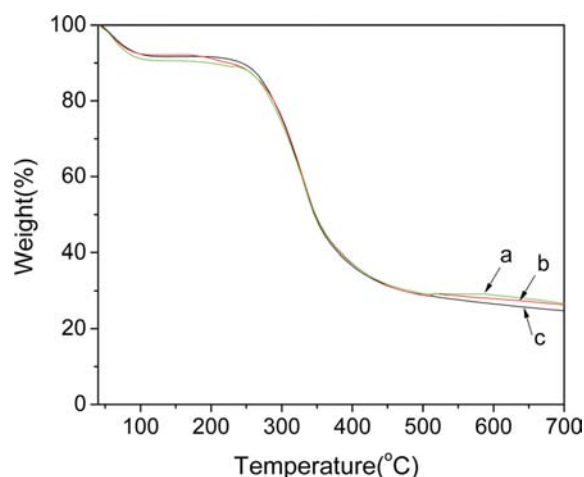


Figure 9. TGA curves of RGO/gelatin composite films with various RGO concentrations of 0.5% (a); 0.3% (b); 0% (c).

Thermal Stability of RGO/Gelatin Nanocomposite Films.

TGA is a standard technique to evaluate the thermal stability of materials. Figure 9 shows the TGA curves of gelatin and the RGO/gelatin composite films in a nitrogen atmosphere. There is a mass loss of about 8% before 100 °C which is assigned to the evaporation of the water in the films. When the temperature is over 250 °C, there is a rapid weight loss, which comes from the thermal degradation of the gelatin. No further large mass losses are observed when the temperature is above 400 °C, and the total weight loss is less than 80%. It seems that the addition of RGO slightly improves the thermal stability of gelatin. In addition, the similar TGA curve shapes for gelatin and RGO/gelatin composite films may suggest the mass loss mainly comes from the gelatin.

Conclusions

RGO was successfully fabricated using gelatin as a reductant. RGO/gelatin composite films with varying RGO contents have been prepared and characterized by SEM, DSC and TGA. The RGO was well dispersed in polymer matrix. The addition of RGO increased the degree of crosslinking of gelatin films and decreased the swelling ability of the gelatin films in water, indicating that RGO/gelatin composite films have a better wet stability than that of gelatin films. The incorporation of RGO also increased the glass transition temperature of gelatin films. The improvement of T_g shows the presence of RGO significantly hinders the mobility of the adsorbed gelatin chains due to the preferable interfacial interactions between the RGO and the polar groups of gelatin. The addition of RGO slightly increases the thermal stability of gelatin films due to the very low content of RGO in the composite films. Since gelatin is a natural and nontoxic polymer with good biocompatibility, the RGO/gelatin composite films are expected to have potential applications in biomedical/biomedicine fields.

Acknowledgments: The work was financially supported by the Project of Shandong Province Higher Educational Science and Technology Program (No. J11LB13).

References

1. S. Liu, N. H. Low, and M. T. Nickerson, *J. Am. Oil Chem. Soc.*, **87**, 809 (2010).
2. H. Ai, S. A. Jones, M. M. Villiers, and Y. M. Lvov, *J. Control. Release*, **86**, 59 (2003).
3. M. Schreiner, S. Huyskens-Keil, A. Krumbein, H. Prono-Widayat, and P. J. Ludders, *Food Eng.*, **56**, 237 (2003).
4. E. Chiellini, P. Cinelli, A. Corti, and E. Kenawy, *Polym. Degrad. Stab.*, **73**, 549 (2001).
5. E. Chiellini, P. Cinelli, E. G. Fernandes, E. R. Kenawy, and A. Lazzeri, *Biomacromolecules*, **2**, 806 (2001).
6. C. Schonauer, E. Tessitore, G. Barbagallo, V. Albanese, and A. Moraci, *Eur. Spine J.*, **13**, 89 (2004).
7. B. Balakrishnan, M. Mohanty, P. R. Umashankar, and A. Jayakrishnan, *Biomaterials*, **26**, 6335 (2005).
8. A. K. Geim and K. S. Novoselov, *Nat. Mater.*, **6**, 183 (2007).
9. C. Lee, X. D. Wei, J. W. Kysar, and J. Hone, *Science*, **321**, 385 (2008).
10. H. Kim, A. A. Abdala, and C. W. Macosko, *Macromolecules*, **43**, 6515 (2010).
11. T. Kuila, S. Bhadra, D. H. Yao, N. H. Kim, B. Sose, and J. H. Lee, *Prog. Polym. Sci.*, **35**, 1350 (2001).
12. C. Shan, H. Yang, J. Song, D. Han, A. Ivaska, and L. Niu, *Anal. Chem.*, **81**, 2378 (2009).
13. H. G. Moon and J. H. Chang, *Polymer(Korea)*, **35**, 265 (2011).
14. W. R. Yang, R. K. Ratinac, S. P. Ringer, P. J. Thordarson, J. Gooding, and F. Braet, *Angew. Chem. Int. Ed.*, **49**, 2114 (2010).
15. T. Ramanathan, A. A. Abdala, S. Stankovich, D. A. Dikin, M. Herrera-Alonso, R. D. Piner, D. H. Adamson, H. C. Schniepp, X. Chen, R. S. Ruoff, S. T. Nguyen, I. A. Aksay, R. K. Prud'Homme, and L. C. Brinson, *Nat. Nanotechnol.*, **3**, 327 (2008).
16. X. M. Yang, Y. F. Tu, L. Li, S. M. Shang, and X. M. Tao, *ACS Appl. Mater. Interfaces*, **2**, 1707 (2010).
17. Y. X. Xu, W. J. Hong, H. Bai, C. Li, and G. Q. Shi, *Carbon*, **47**, 3538 (2009).
18. M. A. Rafiee, J. Rafiee, Z. Wang, H. H. Song, Z. Z. Yu, and N. Koratkar, *ACS Nano*, **3**, 3884 (2009).
19. C. Y. Wan, M. Frydrych, and B. Q. Chen, *Soft Matter*, **7**, 6159 (2011).
20. W. C. Wang, Z. P. Wang, Y. Liu, N. Li, W. Wang, and J. P. Gao, *Mater. Res. Bull.*, **47**, 2245 (2012).
21. W. S. Hummers and R. E. Offeman, *J. Am. Chem. Soc.*, **80**, 1339 (1958).
22. M. Hirata, T. Gotou, S. Horiuchi, M. Fujiwara, and M. Ohba, *Carbon*, **42**, 2929 (2004).
23. J. An, Y. Q. Gou, C. X. Yang, F. D. Hu, and C. M. Wang, *Mater. Sci. Eng. C*, **33**, 2827 (2013).
24. D. Y. Lee, Z. Khatun, J. H. Lee, and Y. K. Lee, *Biomacromolecules*, **12**, 336 (2011).
25. C. S. Shan, H. F. Yang, D. X. Han, Q. X. Zhang, A. Ivaska, and L. Niu, *Langmuir*, **25**, 12030 (2009).
26. R. S. Lakes, *Nature*, **414**, 503 (2001).
27. E. J. Garboczi, J. F. Douglas, and R. B. Bahn, *Mech. Mater.*, **38**, 786 (2006).
28. J. L. Suter and P. V. Coveney, *Soft Matter*, **5**, 3896 (2009).
29. A. Higuchi, J. Komiyama, and T. Lijima, *Polym. Bull.*, **11**, 203 (1984).
30. F. X. Quinn, E. Kampff, G. Smyth, and V. J. McBrierty, *Macromolecules*, **21**, 3191 (1988).